



Influences of Polyvinyl Alcohol Fiber Addition on the Specimen Size Effect and Energy Absorption of Self-Consolidating Concrete

Abbasi Nattaj Omrani, I.¹, Ardeshir-Behrestaghi, A.^{2*} and Saeedian, A.¹

¹ M.Sc., Department of Civil Engineering, Mazandaran University of Science and Technology, Babol, Iran.

² Assistant Professor, Department of Civil Engineering, Mazandaran University of Science and Technology, Babol, Iran.

© University of Tehran 2021

Received: 19 Sep. 2020;

Revised: 23 Jan. 2021;

Accepted: 30 Jan. 2021

ABSTRACT: Polyvinyl alcohol is one of the most efficient synthetic fibers in concrete technology; however, the size effect was rarely evaluated in Polyvinyl alcohol fiber-reinforced concretes. In this research, six types of SCC mixtures containing two dosages of PVA fibers were designed in two strength levels and different sizes of cylindrical specimens were cast. The fresh properties, 28-day compressive strength, and pre-peak energy per unit volume of PVA-FRSCC were evaluated through laboratory tests. Several theoretical models, including Size Effect Law, Modified Size Effect Law, Multi-fractal Scaling Law, and Sim et al. model, were also refined to study the size effect in the designed mixtures under uniaxial compressive failure. Based on the obtained results, the inclusion of Polyvinyl alcohol fibers had significant effect on the performance of the designed concretes. The incorporation of PVA fibers reduced the specimen size effect and improved the ductility and pre-peak energy absorption of plain SCC.

Keywords: Compressive Strength, Energy Absorption, Polyvinyl Alcohol Fiber, Self-Consolidating Concrete, Size Effect.

1. Introduction

Poor tensile strength and inadequate resistance to cracking are the main defects of conventional concrete. These weaknesses are caused by the propagation of micro cracks under the gradual variation of environment and applied loads (Juarez et al., 2015). Internal micro cracks are formed at the mortar-aggregate interface and initiate the brittle behavior of concrete structures (Jebli et al., 2018). It has been shown that the inclusion of randomly distributed fibers can reduce the above

mentioned problems and improve the mechanical characteristics of concrete by bridging the micro cracks (Li et al., 2018; Chang et al., 2020; Sobhani and Pourkhorshidi, 2021). Ramezani and Esfahani (2018) showed that the addition of the optimum amount of steel fibers, alongside with Polypropylene fibers, can enhance the durability and scaling resistance of concretes subjected to cold weather environments.

Polyvinyl alcohol (PVA) is a hydrophilic synthetic fiber that forms a strong connection with the hydrated Portland

* Corresponding author E-mail: ardashir_b_eng@yahoo.com

cement and obtains a noticeable tensile strength, ranging from 880 to 1600 MPa (Si et al., 2020; Ling et al., 2020). Several research studies have focused on the incorporation of PVA fibers in Engineered Cementitious Composites (ECC) (Arain et al., 2019; Zhang and Zhang, 2018; Wang et al., 2020), and structural concretes (Wang et al., 2017; Nuruddin et al., 2015; Xie et al., 2018). According to the mentioned studies, PVA fibers applied noteworthy improvements on the mechanical performance and ductility of concrete. Despite improving these aspects, the addition of synthetic fibers decreases the homogeneity and fluidity of concrete, and causes obstacles in the consolidation process of fresh concrete (Cao et al., 2017).

On the other hand, the durability and mechanical distinction of Fiber-Reinforced Concrete (FRC) can be hampered by improper compaction, which also interrupts the uniform dispersion of fibers. Thus, it is necessary for FRC to obtain a sufficient viscosity and eliminate the demand for mechanical vibration in its consolidation process. Self-Consolidating Concrete (SCC) has managed to push the boundaries and solve the mentioned problems. Unlike conventional concrete, SCC is a highly-workable concrete that compacts itself without utilizing mechanical vibration and flows through the cramped spaces between congested reinforcements in complex formworks (Si et al., 2018).

The synergy between SCC and FRC, called Fiber-Reinforced Self-Consolidating Concrete (FRSCC), merges the rheological stability of SCC with the mechanical advantages of FRC, and eliminate the need for external vibration. In this type of concrete, fiber volume fraction connects the fresh and hardened properties of the material. Therefore, obtaining the optimum fiber volume fraction is one of the most important parameters of FRSCC mixtures (Ferrara et al., 2012).

The dissimilarity between the compressive strength of laboratory size specimens and larger structural elements is

another fundamental challenge. Heterogeneous quasi-brittle materials like concrete, are affected by the size effect phenomenon due to the energy released in the Fracture Process Zone (FPZ), which unlike the Linear Elastic Fracture Mechanics (LEFM), is large and full of cracks. The non-linear behavior of concrete in this large inelastic zone indicates that its nominal compressive strength is influenced by both shape and size of the specimen (Bazant and Oh, 1983).

According to the size effect phenomenon, smaller samples achieve higher strength compared with larger specimens. Based on the fracture mechanics, Bazant (1984) presented a theoretical model, called Size Effect Law (SEL), for specimens with equivalent shapes and crack lengths as follows:

$$f_c(D) = \frac{B f_{cs}}{\sqrt{1 + \frac{D}{D_0}}} \quad (1)$$

where $f_c(D)$: is the compressive strength of specimen, f_{cs} : is the compressive strength of standard cylindrical (150 × 300 mm) or cubic (150 × 150 × 150 mm) specimen, D : is the specimen diameter, and B and D_0 : are to be accomplished via regression analysis as the experimental coefficients.

By adding a size-independent parameter to the Bazant model, Kim and Eo (1990) developed the SEL and proposed the Modified Size Effect Law (MSEL) based on the non-linear fracture mechanics. They indicated that versus the Bazant model, large structural members without initial cracks can withstand stress; therefore, specimens with equivalent shapes and varying initial cracks were examined. MSEL is:

$$f_c(D) = \frac{B f_{cs}}{\sqrt{1 + \frac{D}{D_0}}} + C f_{cs} \quad (2)$$

where B , C , and D_0 : are to be accomplished via regression analysis as the experimental coefficients.

Based on the fractal nature of concrete microstructure, Carpinteri and Chiaia (1997) presented a theoretical model, called Multifractal Scaling Law (MFSL). They indicated that the impacts of material disarray on the mechanical characteristics of concrete diminished, as the specimen diameter increased. They proposed the MFSL model as follows:

$$f_c(D) = f_{c_{\infty}} \sqrt{1 + \frac{L_{ch}}{D}} \quad (3)$$

where $f_{c_{\infty}}$ and L_{ch} : are to be accomplished via regression analysis as the experimental coefficients.

Sim et al. (2013) considered more operative elements like the aspect ratio and unit weight of concrete, and presented a new theoretical model. They reported that the size effect vanished, as the unit weight of concrete increased. Their model is:

$$f_c(D) = \frac{A \sqrt{n_1^{X_4}}}{\sqrt{1 + B D \left(\frac{\rho_c}{\rho_0}\right)^{-X_2}}} f_{cs} + C f_{cs} \quad (4)$$

where ρ_0 : is the unit weight of normal weight concrete, equals to 2300 kg/m^3 , and A, B, C, X_2 , and X_4 : are to be accomplished via regression analysis as the experimental coefficients.

Some of these models were originally designed to assess the size effect in tensile failure; however, the ultimate failure of specimens under uniaxial compression is also caused by the propagation of macro-cracks, implying Mode I failure. Thus, through considering the compressive strength of standard specimens, the mentioned models can be applied for the compressive failure of concretes without initial notch (Asadollahi et al., 2016).

The purpose of this research is to conduct an experimental and numerical investigation to evaluate the impacts of PVA fiber addition on the fresh properties, 28-day compressive strength, specimen size effect, and pre-peak behavior of self-consolidating concrete.

The permeability characteristics and

mechanical behavior of concretes, containing alternative aggregates and fibers, have been studied before in the pre-peak region of stress-strain curves (Prathipati et al., 2020; Cui et al., 2012). In this study, the effect of PVA fibers on the pre-peak performance of SCC is assessed under compression. Also, the empirical coefficients of several size effect models, including SEL, MSEL, MFSL, and Sim et al. (2013) model, were obtained via regression analysis for PVA-FRSCC mixtures.

2. Materials and Methods

2.1. Cement and Aggregates

The utilized fine particles are type II Portland cement, conforming to ASTM C150 (ASTM, 2002), natural river sand with bulk specific gravity and water absorption of 2.63 and 1.95%, respectively, and limestone powder, as the filler material (Madani et al., 2016). The used coarse aggregate was also provided from a local river, having a bulk specific gravity of 2.67, water absorption of 1.3%, and the maximum size of 12.5 mm, conforming to ASTM C33 (ASTM, 2003). Figures 1 and 2 illustrate the gradation of the fine and coarse aggregates, respectively.

2.2. Fiber and Chemical Admixtures

In order to attain a fluid SCC, high-performance poly-carboxylate superplasticizer was used in all mixtures. The utilized water was clean tap water. As one of the main factors of FRSCC mixtures, fiber volume fractions were carefully designed after conducting several experiments. Polyvinyl alcohol fiber with a length of 6 mm and volume fractions of 0.05% and 0.08% was used in the designed mixtures. The utilized fibers were manufactured at Anhui Wanwei group Co. No surface pre-treatment was conducted on the fibers, to maintain the fiber/mortar bonding quality. The mechanical properties of polyvinyl alcohol fiber are given in Table 1 (Hossain et al., 2013). Figure 3 shows the image of the fiber.

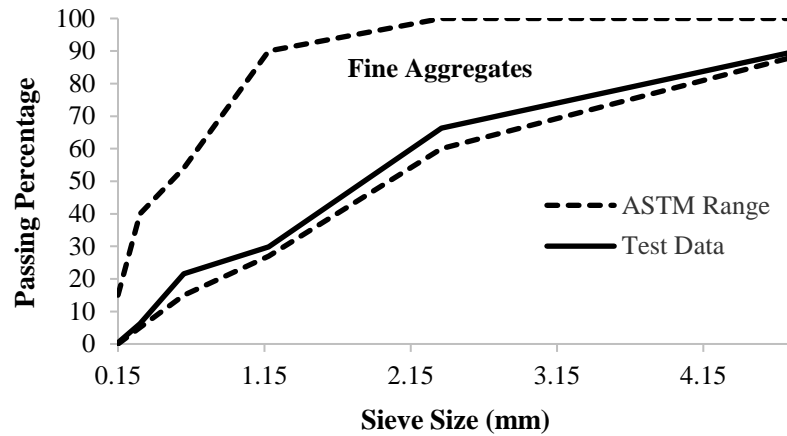


Fig. 1. Gradation of the utilized fine aggregates

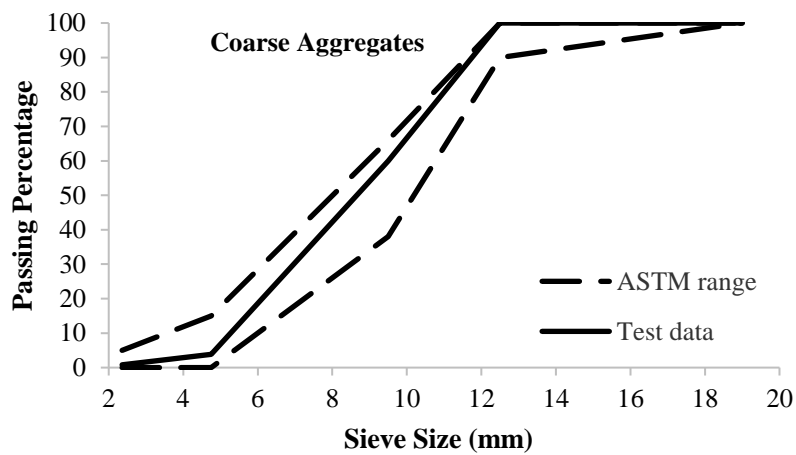


Fig. 2. Gradation of the utilized coarse aggregates



Fig. 3. Polyvinyl alcohol fiber with a length of 6 mm

Table 1. Properties of PVA fibers (Hossain et al., 2013)

Property	PVA fiber
Density (kg/m^3)	1300
Young's modulus (GPa)	32
Length (mm)	6
Diameter (mm)	0.04
Tensile strength (MPa)	1400
Elongation capacity (%)	7

2.3. Mixture Procedure

An experimental process was carried out to design the optimal mix proportions. Six types of FRSCC mixtures containing two different dosages of PVA fibers were created in two strength classes, including LSCC, LSCC-PVA-0.05, LSCC-PVA-0.08, MSCC, MSCC-PVA-0.05, and MSCC-PVA-0.08, where LSCC and MSCC stand for low strength SCC and medium strength SCC, respectively. The exact mix proportions are provided in Table 2.

Although higher dosages of PVA fibers were used in other cementitious composites, the incorporation of these hydrophilic fibers in self-consolidating concretes must be limited due to the specific requirements of SCC at the fresh state. It was reported that the inclusion of 0.15% and 0.2% of PVA fibers can cause serious decrease in the workability and fluidity of self-consolidating concrete (Hossain et al., 2012). The mentioned report has been proven through the experimental phase of this research. At first, 0.15% and 0.2% of PVA fibers were included into the matrix; however, noticeable decrease in the flowability of concrete was observed, and the fresh properties of these mixtures did not reach the self-consolidating criteria. Also, this obstacle could not be solved through increasing the amount of superplasticizer or heightening the W/C ratio, because increasing the amount of these elements can compromise the homogeneity of the system. After trying several fiber dosages, the optimum volumes of PVA fibers were achieved in this study.

In addition, the incorporation of these low volumes of PVA fibers can still imply noticeable effect on the hardened behavior of SCC. For example, it was reported that the addition of 0.125% of PVA fibers increased the 28-day splitting tensile and flexural strength of SCC by 44.4% and 26.4%, respectively (Hossain et al., 2013).

The W/C ratios of the plain mixtures and fiber-reinforced mixtures were kept similar; however, higher amounts of cement and water were utilized in fiber-reinforced

mixtures in an analogous way, to provide the suitable hydration process of cementitious particles. It was observed that low water and cement content can cause serious segregation in fiber-reinforced mixtures. This phenomenon is due to the hydrophilic properties of PVA fibers. Thus, the optimum amounts of water and cementitious particles were included in PVA fiber-reinforced mixtures to prevent segregation and control the presence of PVA fibers inside the matrix.

Ninety cylindrical (Cy) specimens with three different diameters of 75, 100, and 150 mm, and an aspect ratio (height/diameter) of 2, were cast. A laboratory concrete mixer was used to prepare the FRSCC mixtures. First, the natural river sand and coarse aggregates were mixed for 10 seconds. Then, the combination of cement and limestone powder was added into the mixture, and after mixing for 30 seconds, 65% of the total volume of plain water was dispersed throughout the mixture, and mixing continued for another 30 seconds. Afterwards, the residual water containing the whole superplasticizer was included and stirring was continued for 1 minute. After stopping for 10 seconds, PVA fibers were distributed gradually into the mixture and blended for 2 minutes to achieve a homogeneous fiber-reinforced SCC.

2.4. Curing Process and Preparation for Testing

Once the mixing operation was over, fresh concrete tests were carried out to examine the fresh stability of SCC before and after the addition of PVA fibers. The mentioned tests were slump flow time and diameter, V-funnel flow time, and L-box, conforming to EFNARC (2005) and ACI 237R (ACI, 2007). The obtained results of these tests can assess the fluidity, segregation resistance, filling ability, and passing ability of fresh concrete in restricted and unconfined conditions (EFNARC, 2005).

Table 2. Mix proportions of PVA-FRSCC mixtures (kg/m³)

Mixing schemes	Water	Cement	W/C	Fine agg.	Coarse agg.	Limestone powder	Super plasticizer	Fibers
LSCC	192	400	0.48	850	667	215	6.5	---
LSCC-PVA-0.05	240	500	0.48	850	667	215	8.125	0.65
LSCC-PVA-0.08	240	500	0.48	850	667	215	8.125	1.04
MSCC	178.6	470	0.38	800	667	215	12	---
MSCC-PVA-0.05	226.6	596.3	0.38	800	667	215	15.2	0.65
MSCC-PVA-0.08	226.6	596.3	0.38	800	667	215	15.2	1.04

After conducting the fresh concrete tests, cylindrical specimens were cast without any external vibration. The samples were demolded after 24 hrs of casting and cured in a water pool until the required duration of the compressive strength test, conforming to ASTM C192 (ASTM, 2006a). After 28 days of curing, neoprene pads were used to cap the specimens, according to ASTM C1231 (ASTM, 2006b), and the compressive strength test was operated by using a 200-KN pressure jack, conforming to ASTM C39 (ASTM, 2006c). In these tests, the axial load was applied at the rate of 3 kN/s. Figure 4 shows the symbolic failure mode of cylindrical specimens.

3. Results and Discussions

3.1. Fresh Properties

Fresh properties of the PVA-FRSCC mixtures are given in Table 3. According to the Slump flow time (T_{500} time) test results, the incorporation of 0.05% and 0.08% of PVA fibers increased the recorded time for low strength SCC by 27.14% and 65%,

respectively, and increased the recorded time for medium strength SCC by 5.67% and 21.27%, respectively. According to the results of the Slump flow diameter test, the inclusion of 0.05% and 0.08% of PVA fibers lessened the fluidity of low strength SCC by 4.42% and 21.4%, respectively, and lowered the fluidity of medium strength SCC by 6.87% and 19.37%, respectively. LSCC-PVA-0.08 had the lowest fluidity among the mixtures, reaching a diameter of about 532 mm, while the least approved value of spread for SCC is supposed to be 550 mm (EFNARC, 2005).

The results of the V-funnel flow time test showed that all mixtures met the requirements of SCC (6 s to 12 s), and obtained a sufficient segregation resistance (EFNARC, 2005). According to the test results, the addition of 0.05% and 0.08% of PVA fibers decreased the filling ability of low strength SCC by 5.7% and 12.58%, respectively, and lessened the filling ability of medium strength SCC by 1.97% and 9.7%, respectively.



Fig. 4. Typical crack pattern of failed cylindrical specimens

Table 3. Fresh properties of PVA-FRSCC mixtures

Mixing schemes	Slump flow		V-funnel (s)	L-box (H_2/H_1)
	T_{500} (s)	D-final (mm)		
LSCC	1.4	677	8.42	0.8
LSCC-PVA-0.05	1.78	647	8.9	0.76
LSCC-PVA-0.08	2.31	532	9.48	0.68
MSCC	4.23	716	10.61	0.85
MSCC-PVA-0.05	4.47	667	10.82	0.83
MSCC-PVA-0.08	5.13	577	11.64	0.78

Based on the L-box test results, the inclusion of 0.05% and 0.08% of PVA fibers decreased the passing ability of low strength SCC by 5% and 15%, respectively, and lowered the passing ability of medium strength SCC by 2.35% and 8.23%, respectively. Except for LSCC, MSCC, and MSCC-PVA-0.05, other mixtures did not achieve the approved L-box index for SCC, which is 0.8 (EFNARC, 2005).

As expected, the hydrophilic nature of PVA fiber causes a reduction in the workability and fluidity of fresh SCC. Moreover, increasing the PVA fiber volume fraction heightens the slump reduction in both low strength and medium strength mixtures. This impact was more significant in low strength mixtures.

3.2. Compressive Strength

The 28-day compressive strength test results for cylindrical specimens are given in Table 4. Increasing the diameter of cylindrical specimens from 75 to 150 mm, lowered the average compressive strength of LSCC, LSCC-PVA-0.05 and LSCC-PVA-0.08 by 19.54%, 17.6% and 12.84%, respectively, and decreased the average compressive strength of MSCC, MSCC-PVA-0.05 and MSCC-PVA-0.08 by 12.56%, 12.65% and 8.55%, respectively. The compressive strength of three samples were studied for each specimen size, and the standard deviation of these data sets are included in Table 4.

Figure 5 illustrates the reduction of compressive strength, as the size of cylindrical specimen increases. As can be observed from Figure 5, the inclusion of PVA fibers lowered the rate of strength reduction and lessened the size effect in cylinders. This effect was more pronounced

in specimens containing 0.08% of PVA fibers. Based on the test results, the inclusion of 0.05% and 0.08% of PVA fibers decreased the rate of the strength reduction of low strength cylinders by 17.19% and 49.07%, respectively, and lowered the rate of the strength reduction of medium strength cylinders by 8.53% and 42.02%, respectively. Consequently, increasing the PVA fiber volume fraction heightens the diminution of the size effect in cylinders. The addition of PVA fibers improves the ductility of the brittle self-consolidating concrete by counteracting the spread of internal micro cracks and creating a well-made connection with the cementitious mortar. Thus, PVA fiber-reinforced SCC can exhibit a better resistance against the size effect.

Table 5 summarizes the equations of strength reduction. Increasing the PVA fiber volume fraction lessened the gradient of these equations, which indicates a reduction in the dependency of the concrete's strength on the specimen size.

As expected from Hossain et al. (2013) results, the compressive strength of cylindrical specimen was decreased by increasing the PVA fiber content. Unlike Khaloo et al. (2014) results, it can be seen from Table 4 that increasing the PVA fiber volume fraction caused a greater rate of strength reduction in medium strength specimens, compared with low strength specimens. It can be assumed that the low amount of water in medium strength specimen allows the hydrophilic PVA fiber to develop higher internal voids that causes a considerable strength reduction.

3.3. Theoretical Analysis of Size Effect

The empirical coefficients of four size

effect models (see Eqs. (1-4)), were achieved through regression analysis, and the mentioned size effect models were refined for the designed concretes. Tables 6 to 9 summarize the results for SEL, MFSL, MSEL and Sim et al. model, respectively. In addition, the correlation coefficients (R^2)

were obtained by utilizing non-linear model fit in Mathematica. As can be observed from these tables, the high values of R^2 demonstrate the efficiency of the refined models in evaluating the size effect of the designed mixtures.

Table 4. Results of the 28-day compressive strength test

Mixing schemes	Size (mm)		Compressive strength (MPa)				Average
	Diameter	Height	Test 1	Test 2	Test 3	Standard deviation	
LSCC	75	150	22.8	28.1	29	2.73	26.6
	100	200	26.1	23.3	25.1	1.58	24.8
	150	300	23.6	19.9	20.8	1.57	21.4
LSCC-PVA-0.05	75	150	29.2	19.9	26	3.85	25
	100	200	23.9	22.4	21	1.18	22.4
	150	300	23.8	18.9	19.1	2.26	20.6
LSCC-PVA-0.08	75	150	22.1	23	20.4	1.07	21.8
	100	200	21.1	18.7	19.4	1	19.7
	150	300	22.1	18.1	17	2.19	19
MSCC	75	150	35.5	34.4	37.6	1.32	35.8
	100	200	36.8	30.8	32.1	2.57	33.2
	150	300	34.6	30.4	29.1	2.34	31.3
MSCC-PVA-0.05	75	150	32.5	31	31.4	0.63	31.6
	100	200	29.6	29.6	30.4	0.37	29.8
	150	300	23.6	28.7	30.5	2.92	27.6
MSCC-PVA-0.08	75	150	30.1	31.9	29.2	1.12	30.4
	100	200	31.3	27.3	27.9	1.76	28.8
	150	300	32	25.1	26.3	3	27.8

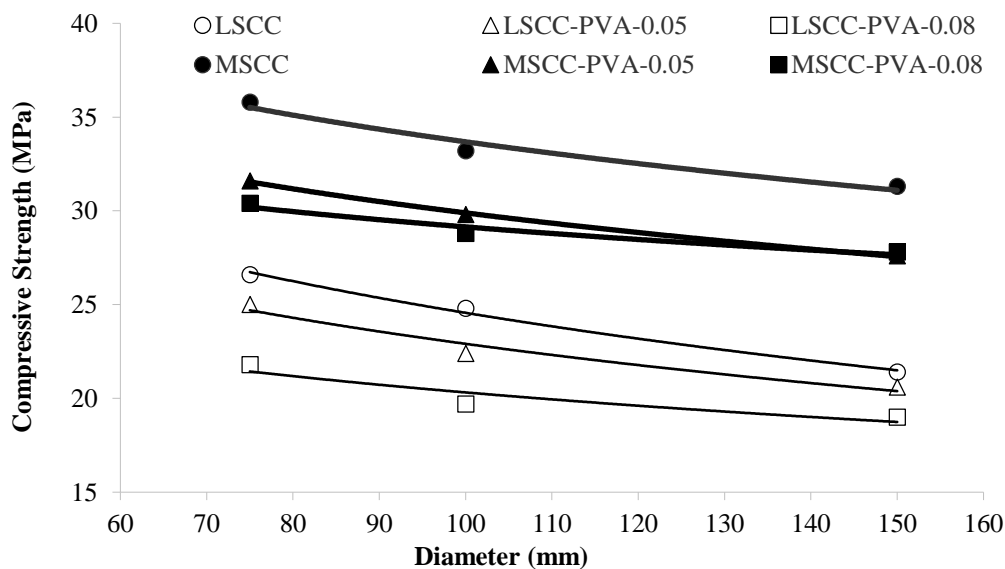


Fig. 5. Compressive strength reduction of low strength and medium strength cylindrical specimens with different diameters

Table 5. Logarithmic equations of strength reduction for different mixes

Mixing schemes	Logarithmic equations
LSCC	$y = -7.56 \ln(x) + 59.379$
LSCC-PVA-0.05	$y = -6.22 \ln(x) + 51.567$
LSCC-PVA-0.08	$y = -3.88 \ln(x) + 38.223$
MSCC	$y = -6.37 \ln(x) + 63.035$
MSCC-PVA-0.05	$y = -5.74 \ln(x) + 56.364$
MSCC-PVA-0.08	$y = -3.66 \ln(x) + 46.031$

Table 6. SEL relation coefficients for different mixes with the use of nonlinear regression analysis

Mixing schemes	Coefficients		
	B	D_0	R^2
LSCC	1.84	63.47	0.99
LSCC-PVA-0.05	1.66	81.25	0.98
LSCC-PVA-0.08	1.35	171.62	0.99
MSCC	1.35	173.97	0.99
MSCC-PVA-0.05	1.37	164.91	0.99
MSCC-PVA-0.08	1.2	319.47	0.99

Table 7. MFSL relation coefficients for different mixes with the use of nonlinear regression analysis

Mixing schemes	Coefficients		
	$f_{c\infty}$	L_{ch}	R^2
LSCC	14.6	179.01	0.99
LSCC-PVA-0.05	14.79	136.66	0.98
LSCC-PVA-0.08	15.62	67.79	0.99
MSCC	26.03	65.85	0.99
MSCC-PVA-0.05	22.91	68.53	0.99
MSCC-PVA-0.08	24.84	36.52	0.99

Table 8. MSEL relation coefficients for different mixes with the use of nonlinear regression analysis

Mixing schemes	Coefficients			
	B	C	D_0	R^2
LSCC	6.68	-5.16	858.5	0.99
LSCC-PVA-0.05	30.64	0.47	0.042	0.98
LSCC-PVA-0.08	24.6	0.64	0.029	0.99
MSCC	17.75	0.65	0.055	0.99
MSCC-PVA-0.05	1.28	0.57	18.47	0.99
MSCC-PVA-0.08	11.66	0.77	0.055	0.99

Table 9. Chemical and physical properties of natural zeolite according to ASTM C618

Mixing schemes	Coefficients					
	A	B	C	X_2	X_4	R^2
LSCC	1.17	0.11	0.02	145.8	1.31	0.99
LSCC-PVA-0.05	4.92	2.57	0.47	-107.91	13.86	0.98
LSCC-PVA-0.08	6.71	4.9	0.64	-263.55	29.78	0.99
MSCC	569.62	46.87	1.06	-14048.9	-1208.76	0.99
MSCC-PVA-0.05	0.95	0.24	0.57	16.43	0.85	0.99
MSCC-PVA-0.08	6.2	9.56	0.77	-107.07	15.08	0.99

Figures 6a and 6b assess the effects of PVA fiber addition on the SEL results of low strength and medium strength cylinders. The mentioned figures indicate that medium strength cylindrical specimens exhibit a greater inclination toward the strength criterion and obtain higher values of transitional size (D_0), compared with low strength cylindrical specimens, conforming to Dehestani et al. (2014) results. Furthermore, the inclusion of PVA fibers lessened the size effect by switching the

SEL results toward the strength criterion. This trend was more significant in mixtures containing 0.08% of fiber content.

Table 10 compares the obtained SEL results with the reported results of Saedian et al. (2017), in order to differentiate between the impacts of PVA fibers and Polypropylene fibers. Based on the data of Table 10, the addition of 0.08% of PVA fibers increased the transitional size of low strength cylinders by 170.39%. Whereas, the incorporation of 0.25% of

Polypropylene fibers, with the length of 6 mm, increased the same aspect in low strength cylinders by 5.22%, in Saeedian et al. (2017) research. Consequently, PVA fibers seem to be more efficient in switching the SEL results of cylindrical specimens toward the strength criterion, compared with Polypropylene fibers.

Figures 7a and 7b display the diagrams of MFSL for cylindrical specimens. Medium strength cylindrical specimens obtained lower values of internal characteristic length (L_{ch}) and had a greater tendency toward the Euclidian regime, compared with low strength cylindrical

specimens. Thus, low strength cylinders show a more brittle behavior. In addition, it can be observed from Figures 7a and 7b that the incorporation of PVA fibers lessened the impacts of specimen size and shifted the MFSL results toward the plastic criterion in both low strength and medium strength cylinders. Also, as expected from the multifractal scaling law, enlarging the specimen size decreased the effects of material disorder in cylinders; meaning that the MFSL results tended to move away from the fractal regime, as the cylinder diameter increased.

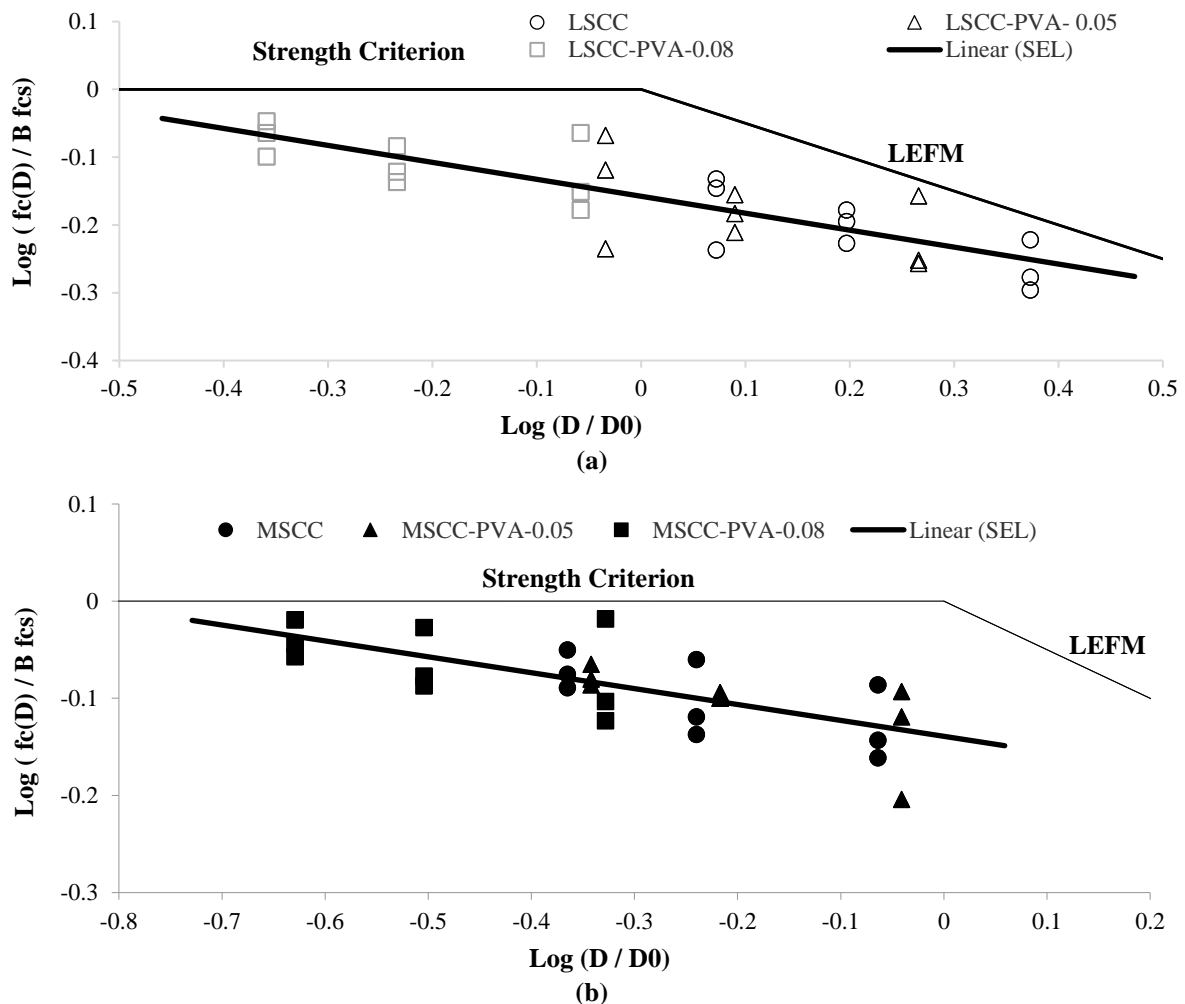


Fig. 6. a) Results of size effect law (SEL) for low strength cylinders; and b) Results of size effect law (SEL) for medium strength cylinders

Table 10. Comparison of transitional size coefficient (D_0) in the present study and Saeedian et al. (2017) research

Reference	Fiber type (Length)	Fiber volume fraction	D_0 of SEL	
			Plain LSCC	Fiber reinforced LSCC
Saeedian et al. (2017)	Polypropylene fiber (6 mm)	0.25%	118.72	124.92
The present study	Polyvinyl alcohol fiber (6 mm)	0.08%	63.47	171.62

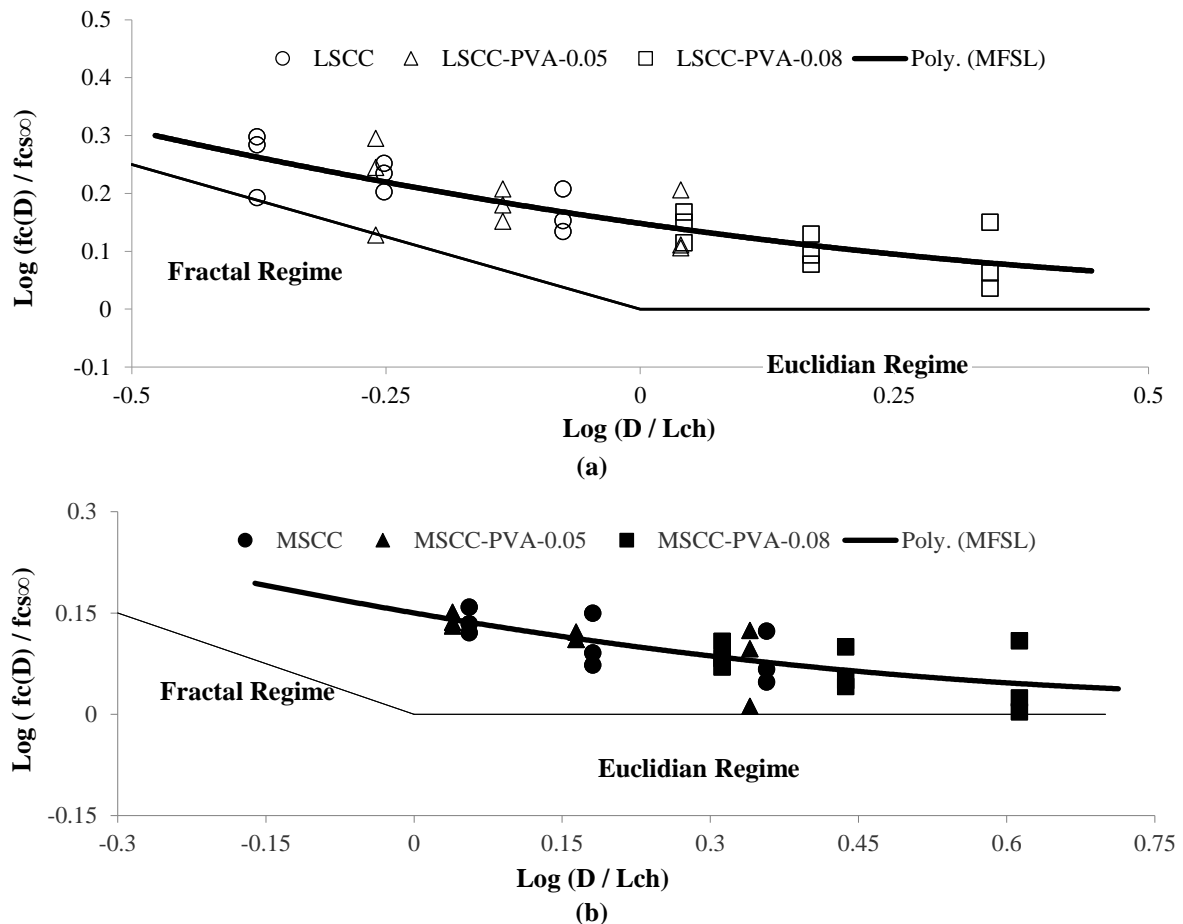


Fig. 7. a) Results of multifractal scaling law (MFSL) for low strength cylinders; and b) Results of multifractal scaling law (MFSL) for medium strength cylinders

Table 11 compares the obtained MFSL results with the reported results of Akbari et al. (2019). As can be observed from this table, the inclusion of 0.3% of steel fibers with a length of 33 mm in Akbari et al. (2019), lessened the internal characteristic length of cylindrical specimens by 49.37%. While, the addition of 0.08% of PVA fibers in the present study decreased the internal characteristic length of medium strength cylinders by 44.54%.

In order to evaluate the credibility of the refined size effect equations, scatter plots of predicted compressive strength versus measured compressive strength are displayed in Figures 8a to 8f. As can be seen from these figures, the predictions of the refined size effect models show an analogous tendency compared to the measured data for all mixtures. Thus, the obtained empirical coefficients of the size effect models, presented in Eqs. (1-4), can analyze the size effect and predict the

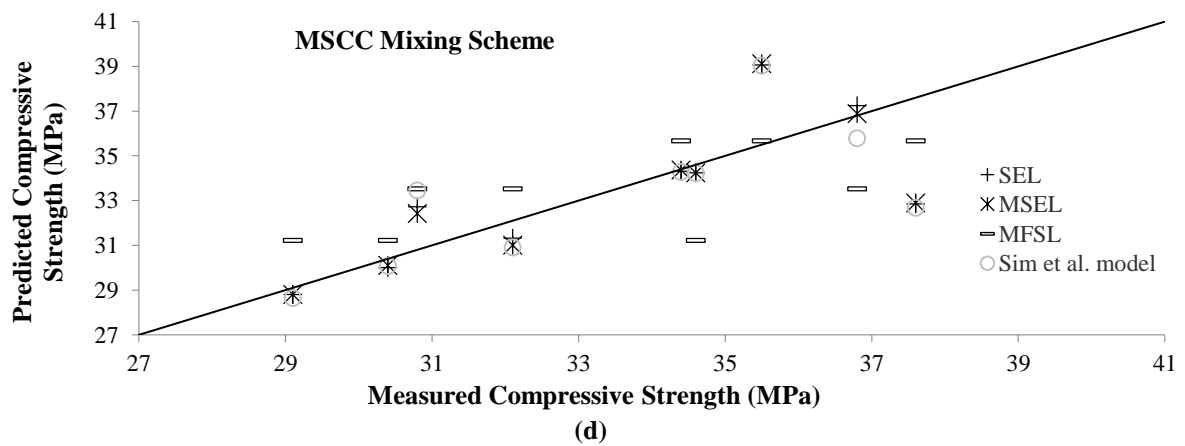
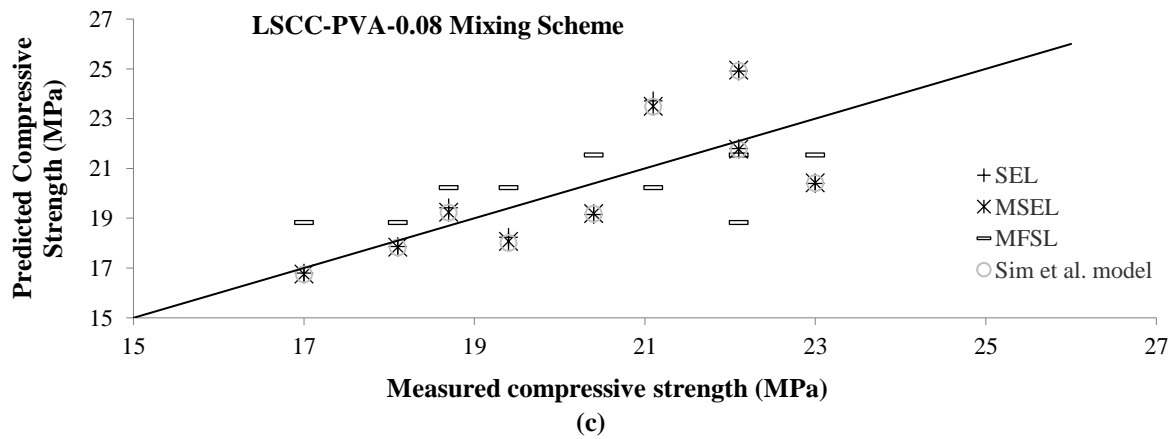
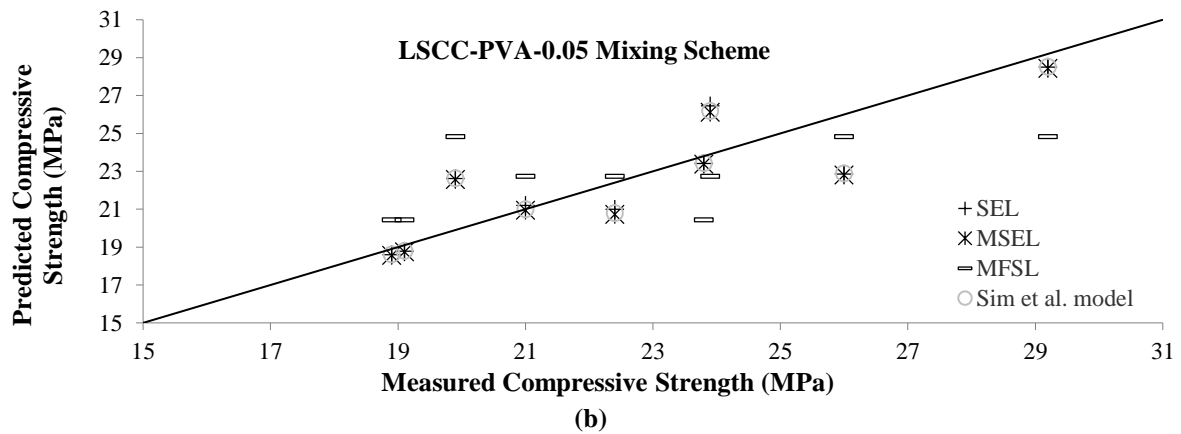
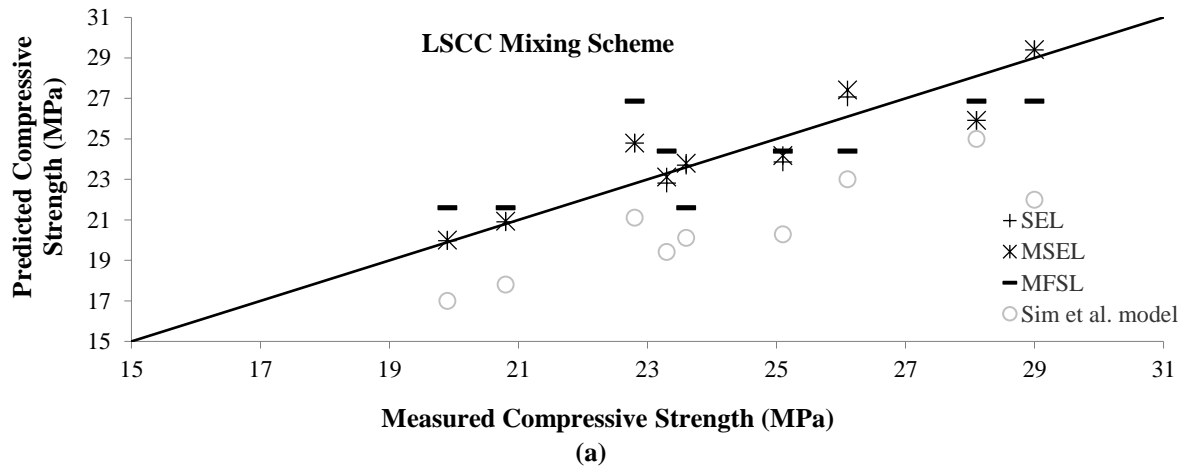
strength for PVA fiber-reinforced self-consolidating concretes.

3.4. Pre-Peak Stress-Strain Curves

Figures 9a and 9b display the pre-peak stress-strain curves of low strength and medium strength standard cylinders under compression, respectively. It has already been reported that the localization of compressive failure and initiation of internal micro cracks gradually begins in the pre-peak portion of stress-strain curve. Through measuring this area, the pre-peak energy per unit volume of concrete can be assessed, which represents the dissipation of energy due to the formation of micro cracks up to peak stress (Jansen and Shah, 1997). The mentioned area was calculated

via $E = \int_0^{\varepsilon} \sigma d\varepsilon$ relation, where E , σ and ε :

represent pre-peak energy absorption, stress and strain, respectively.



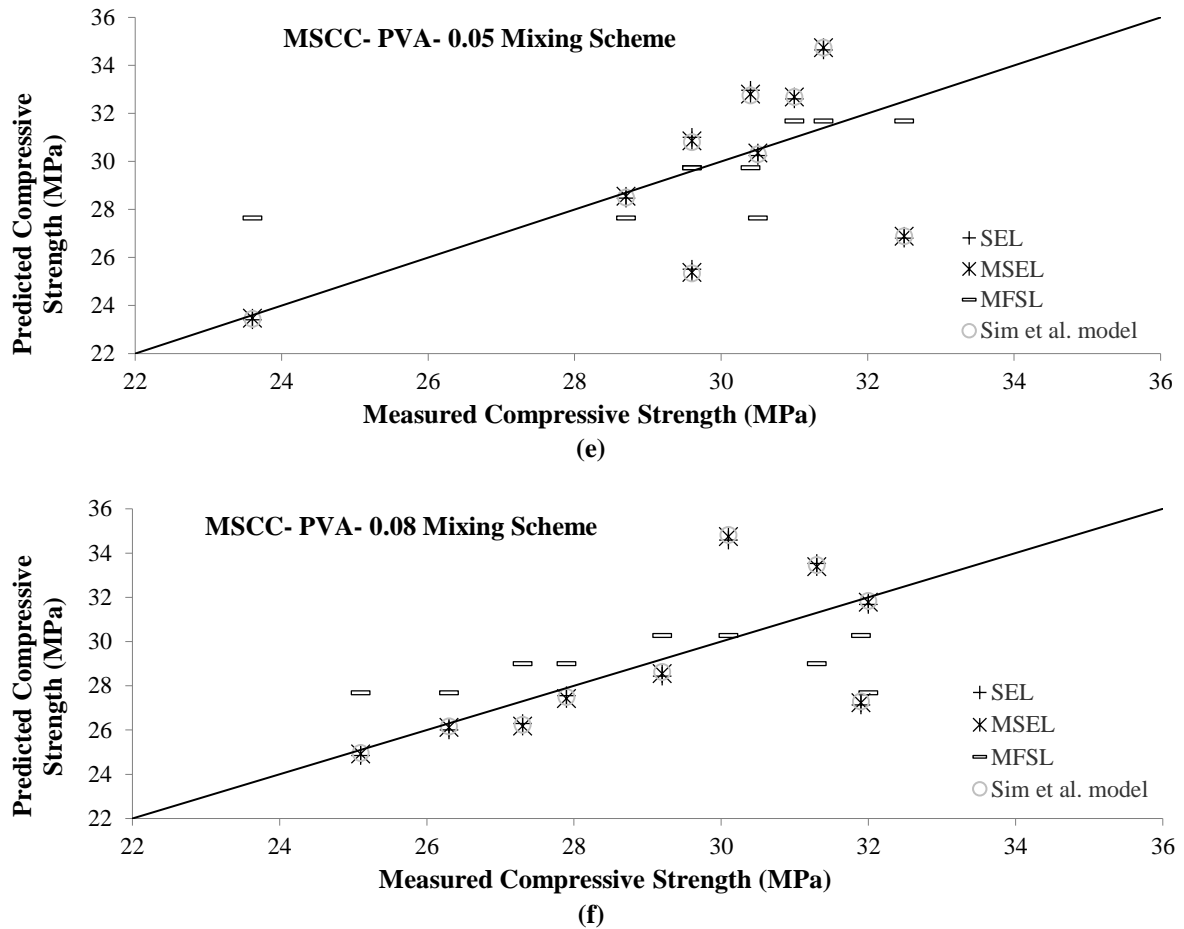


Fig. 8. a) Comparison between the predicted and measured compressive strength results for LSCC mixing scheme; b) Comparison between the predicted and measured compressive strength results for LSCC-PVA-0.05 mixing scheme; c) Comparison between the predicted and measured compressive strength results for LSCC-PVA-0.08 mixing scheme; d) Comparison between the predicted and measured compressive strength results for MSCC mixing scheme; e) Comparison between the predicted and measured compressive strength results for MSCC-PVA-0.05 mixing scheme; and f) Comparison between the predicted and measured compressive strength results for MSCC-PVA-0.08 mixing scheme

Table 11. Comparison of internal characteristic length coefficient (L_{ch}) in the present study and Akbari et al. (2019) research

Reference	Fiber type (Length)	Fiber volume fraction	L_{ch} of MFSL	
			Plain MSCC	Fiber reinforced MSCC
Akbari et al. (2019)	Steel fiber (33mm)	0.3%	86.16	43.62
The present study	Polyvinyl alcohol fiber (6mm)	0.08%	65.85	36.52

As can be seen from Figures 9a and 9b, increasing the PVA fiber content expanded this area for low strength and medium strength cylinders, which indicates an increment in the energy absorption and ductility of concrete in the pre-peak stress-strain portion. The shapes of the fiber-reinforced and plain specimen's curves are mostly linear; however, the stretched strain of fiber-reinforced specimens indicate a higher curvature for fiber-reinforced cylinders at peak stress. Also, the inclusion of PVA fibers increased the strain of

specimens at peak stress, under compressive failure. This trend was more significant in cylinders incorporating 0.08% of PVA fibers. Table 12 reports the impacts of PVA fiber addition on the pre-peak stress-strain characteristics of SCC. Based on the obtained results, the addition of 0.05% and 0.08% of PVA fibers increased the pre-peak energy per unit volume of low strength cylinders by 51.7% and 61.3%, respectively, and heightened the mentioned aspect of medium strength cylinders by 23.3% and 42.5%, respectively.

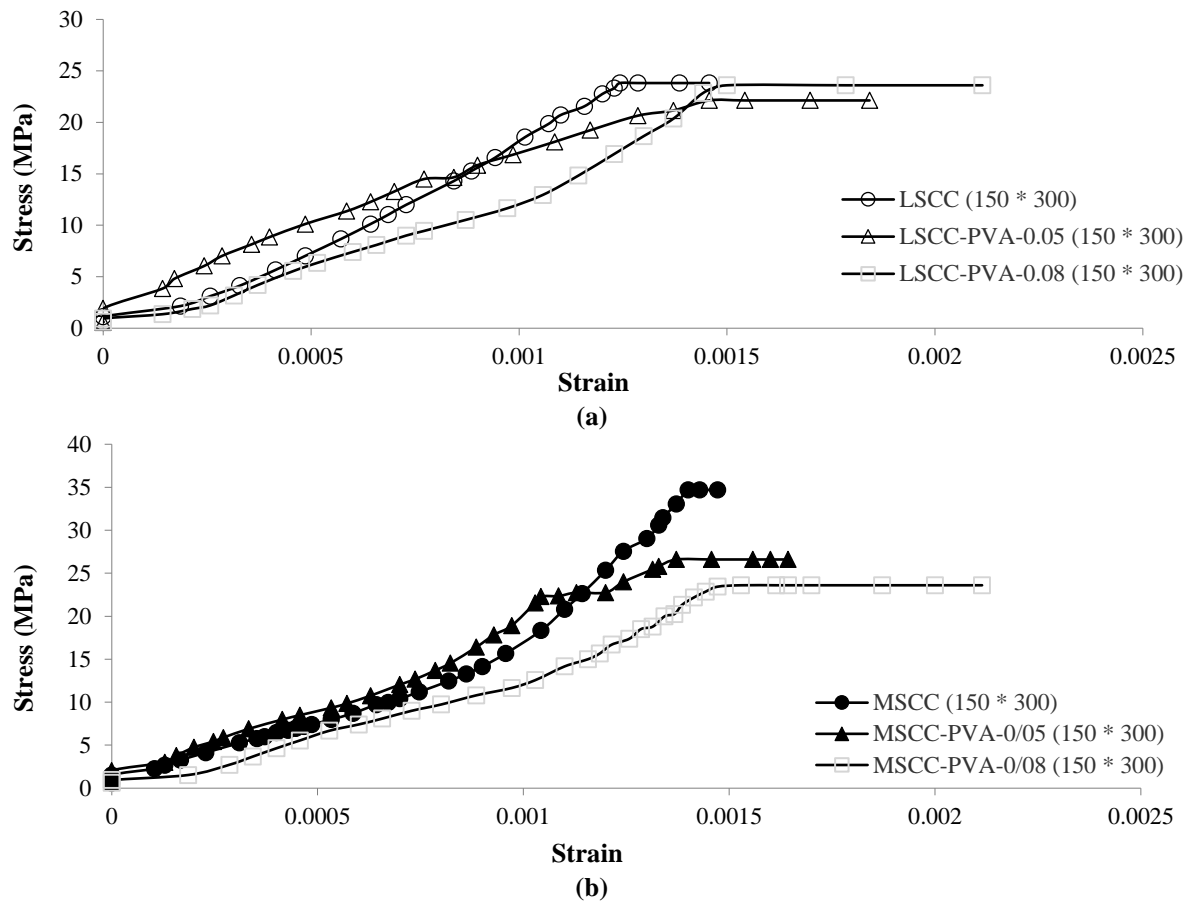


Fig. 9. a) Pre-peak stress-strain curve of low strength cylinders with the diameter of 150 mm containing different dosages of PVA fibers; and b) Pre-peak stress-strain curve of medium strength cylinders with the diameter of 150 mm containing different dosages of PVA fibers

Table 12. Pre-peak energy absorption per unit volume for standard cylinders

Mixing schemes	E (N.mm/mm ³)
LSCC	0.01814
LSCC-PVA-0.05	0.02752
LSCC-PVA-0.08	0.02927
MSCC	0.02058
MSCC-PVA-0.05	0.02539
MSCC-PVA-0.08	0.02933

4. Conclusions

Four theoretical models, including SEL, MSEL, MFSL, and Sim et al. model, were refined to evaluate the size effect in PVA fiber-reinforced SCC mixtures under compression. These conclusions have been drawn:

- All cylindrical specimens exhibited a more ductile behavior after the inclusion of PVA fibers. The addition of 0.08% of PVA fibers lowered the rate of strength reduction in low strength and medium strength cylinders by 49.07% and 42.02%, respectively, as the specimen

diameter increased. Furthermore, the hydrophilic properties of PVA fibers lessened the compressive strength of all samples. This effect was more noteworthy in medium strength specimens containing a lower amount of internal water.

- Increasing the PVA fiber content shifted the SEL results toward the strength criterion and reduced the size effect in cylinders. The addition of 0.08% of PVA fibers heightened the transitional size of low strength cylinders and medium strength cylinders by 170.39% and 83.63%, respectively.

- The MFSL results indicated a more brittle behavior in smaller samples. The incorporation of 0.08% of PVA fiber content lowered the internal characteristic length of low strength cylinders and medium strength cylinders by 62.13% and 44.54%, respectively. PVA fiber-reinforced cylindrical specimens with a W/C ratio of 0.38 attained the least values of internal characteristic length and revealed the best performance against the size effect.
- The pre-peak energy per unit volume of low strength and medium strength standard cylinders were calculated through evaluating the area under the stress-strain curves up to peak stress. According to the obtained results, the inclusion of PVA fibers enhanced the ductility of both low strength and medium strength specimens in the pre-peak portion of stress-strain curve, and increased the strain at peak stress.

5. Acknowledgements

This work was supported by the Civil Engineering Department of Mazandaran University of Science and Technology.

6. References

- ACI (American Concrete Institute). (2007). *Self-consolidating concrete*, ACI 237R-07, Farmington Hills, MI.
- Akbari, M., Khalilpour, S. and Dehestani, M. (2019). "Analysis of material size and shape effects for steel fiber reinforcement self-consolidating concrete", *Engineering Fracture Mechanics*, 206, 46-63.
- Araïn, M.F., Wang, M., Chen, J. and Zhang, H. (2019). "Study on PVA fiber surface modification for strain-hardening cementitious composites (PVA-SHCC)", *Construction and Building Materials*, 197, 107-116.
- Asadollahi, S., Saeedian, A., Dehestani, M. and Zahedi, F. (2016). "Improved compressive fracture models for self-consolidating concrete (SCC)", *Construction and Building Materials*, 123, 473-80.
- ASTM. (2002). *Standard specification for Portland cement*, ASTM C150, West Conshohocken, PA.
- ASTM. (2003). *Standard specification for concrete aggregates*, ASTM C33/C33M-16, West Conshohocken, PA.
- ASTM. (2006a). *Standard practice for making and curing concrete test specimens in the laboratory*, ASTM C192/C192M-02, West Conshohocken, PA.
- ASTM. (2006b). *Standard practice for use of unbonded caps in determination of compressive strength of hardened cylindrical concrete specimens*, ASTM C1231/C1231M-15, West Conshohocken, PA.
- ASTM. (2006c). *Standard test method for compressive strength of cylindrical concrete specimens*, ASTM C39/C39M-16b, West Conshohocken, PA.
- Bažant, Z.P. and Oh, B.H. (1983). "Crack band theory for fracture of concrete", *Matériaux et Construction*, 16(3), 155-177.
- Bažant, Z.P. (1984). "Size effect in blunt fracture: concrete, rock, metal", *Journal of engineering mechanics*, 110(4), 518-535.
- Cao, Q., Cheng, Y., Cao, M. and Gao, Q. (2017). "Workability, strength and shrinkage of fiber reinforced expansive self-consolidating concrete", *Construction and Building Materials*, 131, 178-185.
- Carpinteri, A. and Chiaia, B. (1997). "Multifractal scaling laws in the breaking behavior of disordered materials", *Chaos Solitons Fractals*, 8(2), 135-150.
- Chang, J., Cui, K. and Zhang, Y. (2020). "Effect of hybrid steel fibers on the mechanical performances and microstructure of sulphoaluminate cement-based reactive powder concrete", *Construction and Building Materials*, 261, 120502.
- Cui, H.Z., Lo, T.Y., Memon, S.A., Xing, F. and Shi, X. (2012). "Experimental investigation and development of analytical model for pre-peak stress-strain curve of structural lightweight aggregate concrete", *Construction and Building Materials*, 36, 845-859.
- Dehestani, M., Nikbin, I.M. and Asadollahi, S. (2014). "Effects of specimen shape and size on the compressive strength of self-consolidating concrete (SCC)", *Construction and Building Materials*, 66, 685-691.
- EFNARC (European Federation of National Associations Representing for Concrete). (2005). *Specification and guidelines for self-compacting concrete*, Surrey, U.K.
- Ferrara, L., Bamonte, P., Caverzan, A., Musa, A. and Sanal, I. (2012). "A comprehensive methodology to test the performance of steel fiber reinforced self-compacting concrete (SFR-SCC)", *Construction and Building Materials*, 37, 406-424.
- Hossain, K.M.A., Lachemi, M., Sammour, M. and Sonebi, M. (2013). "Strength and fracture energy characteristics of self-consolidating concrete incorporating polyvinyl alcohol, steel and hybrid

- fibers", *Construction and Building Materials*, 45, 20-29.
- Hossain, K.M.A., Lachemi, M., Sammour, M. and Sonebi, M. (2012). "Influence of Polyvinyl alcohol, steel, and hybrid fibers on fresh and rheological properties of self-consolidating concrete", *Journal of Materials in Civil Engineering*, 24, 1211-1220.
- Jansen, D.C. and Shah, S.P. (1997). "Effect of length on compressive strain softening of concrete", *Journal of Engineering Mechanics*, 123(1), 25-35.
- Jebli, M., Jamin, F., Malachanne, E., Garcia-Diaz, E. and El-Youssoufi, M.F. (2018). "Experimental characterization of mechanical properties of the cement-aggregate interface in concrete", *Construction and Building Materials*, 161, 16-25.
- Juarez, C.A., Fajardo, G., Monroy, S., Duran-Herrera, A., Valdez, P. and Magniont, C. (2015). "Comparative study between natural and PVA fibers to reduce plastic shrinkage cracking in cement-based composite", *Construction and Building Materials*, 91, 164-170.
- Khaloo, A., Raisi, E.M., Hosseini, P. and Tahsiri, H. (2014). "Mechanical performance of self-compacting concrete reinforced with steel fibers", *Construction and Building Materials*, 51, 179-186.
- Kim, J.K. and Eo, S.H. (1990). "Size effect in concrete specimens with dissimilar initial cracks", *Magazine of Concrete Research*, 42(153), 233-238.
- Li, B., Chi, Y., Xu, L., Shi, Y. and Li, C. (2018). "Experimental investigation on the flexural behavior of steel-polypropylene hybrid fiber reinforced concrete", *Construction and Building Materials*, 191, 80-94.
- Ling, Y.F., Zhang, P., Wang, J. and Shi, Y. (2020). "Effect of sand size on mechanical performance of cement-based composite containing PVA fibers and nano-SiO₂", *Materials*, 13(2), 325.
- Madani, H., Ramezani-pour, A.A., Shahbazinia, M., Bokaeian, V. and Ahari, S. (2016). "The influence of ultrafine filler materials on mechanical and durability characteristics of concrete", *Civil Engineering Infrastructures Journal*, 49(2), 251-262.
- Nuruddin, M.F., Ullah Khan, S., Shafiq, N. and Ayub, T. (2015). "Strength prediction models for PVA fiber-reinforced high-strength concrete", *Journal of Materials in Civil Engineering*, 27(12), 04015034.
- Prathipati, S.R.R.T., Rao, C.B.K. and Murthy, N.R.D. (2020). "Mechanical behavior of hybrid fiber reinforced high strength concrete with graded fibers", *International Journal of Engineering*, 33(8), 1465-1471.
- Ramezani, A.R. and Esfahani, M.R. (2018). "Evaluation of hybrid fiber reinforced concrete exposed to severe environmental conditions", *Civil Engineering Infrastructures Journal*, 51(1), 119-130.
- Saedian, A., Dehestani, M., Asadollahi, S. and Vaseghi Amiri, J. (2017). "Effect of specimen size on the compressive behavior of self-consolidating concrete containing polypropylene fibers", *Journal of Materials in Civil Engineering*, 29(11), 04017208.
- Si, R., Wang, J., Guo, S., Dai, Q. and Han, S. (2018). "Evaluation of laboratory performance of self-consolidating concrete with recycled tire rubber", *Journal of Cleaner Production*, 180, 823-831.
- Si, W., Cao, M. and Li, L. (2020). "Establishment of fiber factor for rheological and mechanical performance of polyvinyl alcohol (PVA) fiber reinforced mortar", *Construction and Building Materials*, 265, 120347.
- Sim, J.I., Yang, K.H., Kim, H.Y. and Choi, B.J. (2013). "Size and shape effects on compressive strength of lightweight concrete", *Construction and Building Materials*, 38, 854-864.
- Sobhani, J., Pourkhorshidi, A. (2021). "The effects of cold-drawn crimped-end steel fibers on the mechanical and durability of concrete overlay", *Civil Engineering Infrastructures Journal*, 54(2), 319-330.
- Wang, L., Zhou, S.H., Shi, Y., Tang, S.W. and Chen, E. (2017). "Effect of silica fume and PVA fiber on the abrasion resistance and volume stability of concrete", *Composite Part B: Engineering*, 130, 28-37.
- Wang, Q., Lai, M.H., Zhang, J., Wang, Z. and Ho, J.C.M. (2020). "Greener engineered cementitious composite (ECC), The use of pozzolanic fillers and oiled PVA fibers", *Construction and Building Materials*, 247, 118211.
- Xie, T., Mohamed Ali, M.S., Visintin, P. and Oehlers, D.J. (2018). "Partial interaction model of flexural behavior of PVA fiber-reinforced concrete beams with GFRP bars", *Journal of Composites for Construction*, 22(5), 04018043.
- Zhang, Z. and Zhang, Q. (2018). "Matrix tailoring of Engineered Cementitious Composites (ECC) with non-oil-coated, low tensile strength PVA fiber", *Construction and Building Materials*, 161, 420-431.



This article is an open-access article distributed under the terms and conditions of the Creative Commons Attribution (CC-BY) license.